Biomaterials Science

ROYAL SOCIETY OF CHEMISTRY

COMMUNICATION

View Article Online
View Journal | View Issue

Cite this: *Biomater. Sci.*, 2025, **13**, 5352

Received 21st May 2025,
Accepted 11th August 2025

DOI: 10.1039/d5bm00788g

rsc.li/biomaterials-science

A modular, nanoscale platform for the targeted delivery of camptothecin to cancer cells expressing TAG-72

Reham Hassan,[a] Zirui Zhu,[a] Mingyang Ji,[a] Ziyuan Meng,[a] Emily R. Matas,[a] Damu Sunilkumar,[b] Dario Palmieri,[b] Benjamin A. Conrad,[a] Thomas J. Magliery *[a] and Jon R. Parquette *[a]

A camptothecin (CPT)-dilysine nanotube, stabilized with a layer of polydopamine (PDA), was functionalized on the surface with anti-TAG-72 antibody fragments. Cell viability studies showed that the presence of the targeting anti-TAG-72 scFv significantly enhanced cytotoxicity against TAG-72 positive, LS-174T colon cancer cells, compared with HT-29 cells negative for the antigen.

Nanotechnology-based therapeutics have shown great promise for the treatment of cancer due to their enhanced efficacy and safety compared with current chemotherapy regimens.[1] Delivery vehicles with nanoscale dimensions often benefit from the enhanced permeability and retention (EPR) effect, which allows the drugs to be delivered selectively into tumor cells.[2] However, the delivery of nanoparticles into human tumor tissue *via* the EPR effect is not always clinically successful, compared with animal tumor models.[3] This difficulty in translating research to the clinic emerges from heterogeneity amongst patient populations and tumor types.[2,3] Customizable platforms allow the nanocarrier biointerface to be engineered to overcome the unique biological barriers encountered in specific disease states.[4] Recent advances in nanomaterial synthesis offer the potential for the modular assembly of systems specifically designed to overcome these barriers and optimize therapeutic efficacy.[5–9] The challenge lies in creating predictable strategies to precisely tailor the nanoparticle to target the tumor microenvironment.

The active targeting of solid tumors remains as a critical unmet need for most types of cancer.[10] Targeted modalities include antibody monotherapy, antibody drug conjugates (ADCs),[11] radioimmunotherapy,[12] and chimeric antigen receptor (CAR) T-cell therapy.[13] All are limited most by the properties of the molecular targets; there are few markers that are pervasively present on cancer cells in large amounts but are absent in normal tissues.[14] At best, most are elevated in cancer, putting a floor on the toxicity of a targeted approach. Those that are most selective tend to be applicable to only a small range of tumors, such as HER2 with breast and gastric cancer.[15] For many modalities, like most ADCs and radiotherapies, internalization is essential, and not all receptors are internalized. Conjugating chemotoxic agents or radionuclides requires modifications that often compromise the targeting or physical properties of the antibody. However, ADCs must have specific and high-affinity binding to a suitable, internalized receptor, and drug conjugation has proven challenging both in preserving the antibody and in effective release. A broad range of solid tumors, including most adenocarcinomas like colorectal cancer, pancreatic cancer, and ovarian cancer, have no identified agents that meet the criteria.[16] Tumor associated glycoprotein (TAG)-72 is a mucinous cell-surface glycoprotein that is associated with nearly all adenocarcinomas, but is essentially absent in normal human tissue, making it an excellent targeting molecule.[17] It is shed into the extracellular matrix and some, but little, can be found in the blood, because of the viscous properties of the molecule. TAG-72 does not appear to be internalized, limiting its use as an ADC target, but its accumulation in the tumor matrix makes it excellent for imaging and tumor localization.

Nanoparticle platforms must be modular with respect to size, charge and surface properties because these factors impact the *in vivo* stability, circulation time, clearance and tumor penetration.[18] Additionally, they must remain stable at very low therapeutic concentrations in a rapidly fluctuating, extracellular environment containing salts, serum albumins and the potential for enzymatic degradation.[19,20] We have previously shown that the stability of self-assembled nanostructures was significantly enhanced by polymerization of a thin, conformal coating of polydopamine (PDA) onto the surface.[21] The PDA surface coating exhibits inherent reactivity toward nucleophilic groups,[22] which allows for covalent and ionic bonds to form during the coating process and offers the

[a]*Department of Chemistry and Biochemistry, The Ohio State University, 100 W. 18th Ave., Columbus, Ohio 43210, USA. E-mail: parquette.1@osu.edu, magliery.1@osu.edu*
[b]*A Department of Cancer Biology and Genetics, The Ohio State University, Wexner Medical Center and The James Comprehensive Cancer Center, 460 W. 12th Avenue, Columbus, OH, 43210, USA*

potential for post-polymerization surface functionalization.[23] In this work, we incorporated a single chain variable fragment (scFv) based on the anti-TAG-72 antibody 3E8,[24,25] which is fully humanized and optimized for binding, onto the surface of PDA-coated nanotubes constructed from a dipeptide conjugated to the antitumor topoisomerase I inhibitor camptothecin (CPT) (Fig. 1).

The CPT-nanotube was created by the self-assembly of dipeptide KK(CPT)-NH_2 (**CPT-KK**) in PBS (10 mM) for 24 h.[26] To enhance the stability and to permit surface binding, the nanotubes were coated with a layer of PDA deposited on the surface by the *in situ* polymerization of dopamine (DA) at pH 7.4 (PBS).[27] The slightly basic pH of PBS was sufficient to promote the oxidative self-polymerization of dopamine.[28,29] Therefore, to deposit a conformal coating of PDA on the surface of the nanofibers, a solution of pre-assembled CPT-nanotubes (10 mM, PBS, 24 h) was treated with varying amounts of dopamine hydrochloride (DA) and aged for 24 h. The optimal DA : **CPT-KK** ratio of 5 : 1 was identified by the appearance of PDA nanoparticles in TEM images after deposition at higher ratios, due to excess DA polymerizing in solution (Fig. S1).[30] Comparing TEM images of the nanotubes before and after PDA deposition (**CPT-KK** and **DA/CPT-KK**) did not permit confirmation of the surface coating, due to the wide range of diameter dimensions (80–120 nm) of the starting **CPT-KK** nanotubes (Fig. 2a and b). However, a clear increase in the AFM cross-sectional height profiles from ~4 to ~6.6 nm could be observed after PDA deposition. This height increase indicated a 1.3 nm increase in wall thickness, as the AFM heights reflected twice the wall dimensions of the collapsed double wall of the nanotube structure. To further probe the structure of the PDA-coated nanotubes by XPS, a sample was pelleted by centrifugation (12 100*g*) to remove any remaining PDA nanoparticles. The C1S spectra of **CPT-KK** and **DA/CPT-KK** were fitted to five components assigned to C–C(H) at 285 eV, C–OH/C–N at 286.05 eV, N–C═O at 287.18 eV, O–C═O at 288.4 eV, and CF_3 at 292.5 eV (from $CF_3CO_2^-$ peptide counterions). Comparison of the **CPT-KK** and **DA/CPT-KK** spectra revealed a decrease in the N–C═O peak (12.0 to 8.2%) and an increase in the C–OH/C–N peak 21.8% to 30.8% after deposition, as expected for the structure of PDA (Fig. S2).[22]

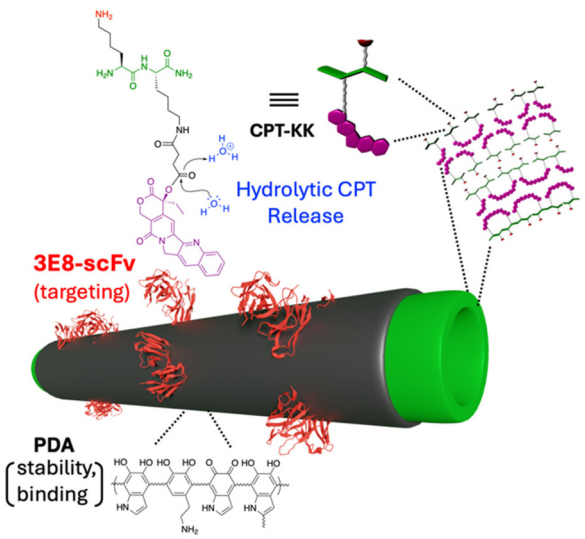

Fig. 1 PDA-coated, CPT-nanotubes with scFv anti-TAG-72 antibody fragments noncovalently bound on the surface showing hydrolysis of ester linkage and CPT release.

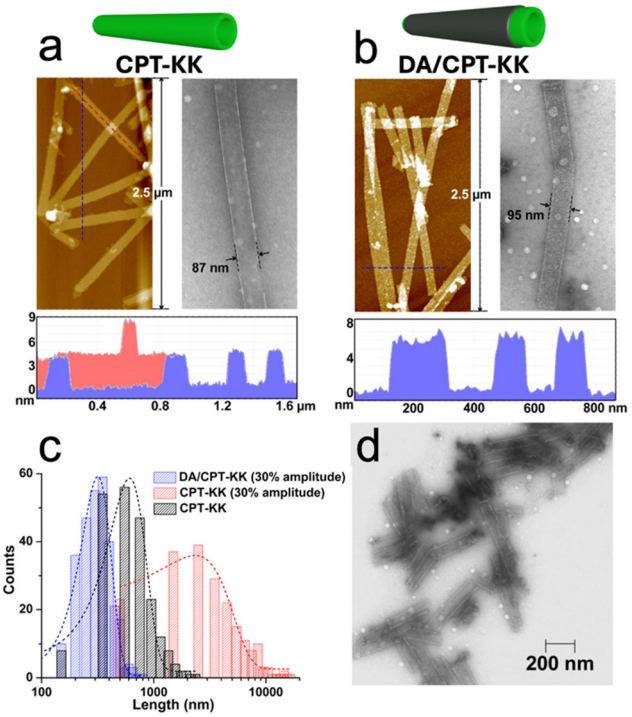

Fig. 2 AFM height profiles and TEM images of (a) **CPT-KK** and (b) **DA/CPT-KK** (5 : 1, n/n) in PBS. After incubation in PBS (10 mM with respect to **CPT-KK**) for 24 h, samples of **CPT-KK** and **DA/CPT-KK** were diluted to 1 mM (PBS) prior to AFM and TEM imaging. After coating **CPT-KK** nanotubes with PDA, the wall thickness increased from 2 nm for **CPT-KK** to ~3.3 nm for **DA/CPT-KK**. (c) Histograms of length distributions, measured from TEM images, of CPT-KK with and without sonication (37.5 W for 1 min) and **DA/CPT-KK** (5 : 1, n/n, sonicated). (d) TEM image of **DA/CPT-KK** after sonication (37.5 W, 1 min).

Many of the factors of nanoparticle delivery, such as biodistribution, circulation time, and cellular uptake, critically depend on size, particularly length.[31–33] Ultrasound-induced shear has been shown to efficiently disperse aggregates and to cut polymers,[34] carbon nanotubes (CNTs)[35,36] and self-assembled nanostructures[37] into smaller fragments. Therefore, sonication was investigated as a strategy to modulate the length of the nanotubes. Deposition of the PDA coating on the surface did not alter the length distribution of the **CPT-KK** nanotubes (Fig. S3). However, sonication (37.5 W, 1 min) of the uncoated **CPT-KK** nanotubes induced elongation of the nanotubes, whereas the same treatment of the PDA-coated nanotubes significantly shortened the nanotubes (Fig. 2c–d, S4). This contrasting behavior emerged from the ability of sonication to induce self-assembly, which would more

profoundly impact the dynamic structures of the **CPT-KK** nanotubes, compared the static PDA-coated system.[38] Importantly, the shortened state of the coated nanotubes persisted, even after 1 week in PBS (10 mM) (Fig. S5). The dynamic structures of self-assembled materials often allow the fragmented structures to regain the prior elongated state. We previously observed that nanotube fragments, shortened by sonication, could be stabilized by polymer-wrapping to slow the self-healing process.[39] Thus, the stability, with respect to elongation, of the shortened states could be attributed to the PDA coating.

Drug release from the PDA-coated nanotubes requires hydrolytic cleavage of the 20-*O*-succinyl linkage. Previously, we found that intact **CPT-KK** nanotubes sequestered the CPT molecules within the hydrophobic walls of the nanotube, thereby rendering the hydrolytic release of CPT, under neutral conditions in PBS, concentration dependent.[26,40] Furthermore, the noncovalent nature of the interactions that stabilize the nanotube structure could be disrupted under physiological conditions. For example, human serum albumin, which is abundant in human serum, has potential to destabilize the nanotubes, leading to more rapid hydrolytic drug release. These factors, along with the presence of hydrolases, would be expected to impact the rate of drug release. The conformal layer of PDA on the CPT-peptide nanotubes stabilized (CMC values of 11 μM for **DA/CPT-KK** *versus* 41 μM for **CPT-KK**) the nanotubes at low concentrations in PBS (Fig. S6). Thus, the presence of the PDA coating could be expected to partially inhibit the rate of CPT release from the nanotubes. To evaluate the impact of the PDA coating, the release rates of **CPT-KK** and **DA/CPT-KK** were measured by HPLC in PBS and HS at 37 °C (Fig. S7–S10). Overall, the PDA coating slightly decreased the release rate compared with the uncoated nanotubes. For example, after incubating in PBS for 83 h at 100 μM, **CPT-KK** and **DA/CPT-KK** released 71% and 57% of the drug, respectively. Hydrolytic degradation and CPT release was significantly faster for both **CPT-KK** and **DA/CPT-KK** in human serum (HS) at 37 °C, releasing 92% and 73% of the drug in 7 h, respectively.[41] These experiments confirm that the presence of the PDA coating only modestly reduced the release rate of CPT, compared with uncoated **CPT-KK** nanotubes.

The surface of the PDA-coated nanotubes was noncovalently functionalized with an scFv of the anti-TAG-72 antibody 3E8, to enhance efficacy against cancer cells positive for TAG-72. The PDA layer exhibits inherent reactivity toward nucleophilic groups, such as amines and thiols, due to the presence of electrophilic catechol quinone components of the coating.[22] This reactivity, along with hydrophobic effects, hydrogen-bonding and ionic interactions, offers the potential to bind the 3E8 scFv on the PDA surface.[23] At a pH of 7.4 in PBS, electrostatic interactions would not significantly contribute to binding due to the low ζ-potential (6.4 mV) of the **DA/CPT-KK** nanotubes. To qualitatively assess the binding of the scFv to the nanotubes, we carried out structured illumination microscopy (SIM) of a sample of **DA/CPT-KK** incubated with fluorescein-labeled scFv after filtration to remove unbound antibody. The nanotubes were then imaged under excitation at 405 and 488 nm, to visualize the CPT within the nanotubes and fluorescein-labelled scFv, respectively. The 405 nm laser only partially overlaps with CPT absorption (λ_{max} ~360 nm), resulting in relatively weak emission of the nanotubes in the SIM images. As shown in Fig. 3, emission signals were detected when **DA/CPT-KK** (without scFv) was excited in the 405 nm (DAPI), but not in the 488 nm (GFP) channel. In contrast, excitation of **DA/CPT-KK**, after incubation with 3E8, produced images in both the 405 and 488 nm channels that colocalized when the images were overlayed. These experiments confirmed that the fluorescent 3E8 scFv co-localized with the nanotubes (Fig. 3) upon binding to the PDA surface of the nanotubes.

To estimate the affinity of the scFv for the nanotubes, we incubated the fluorescein-labeled scFv (2.5 μM) with a range of concentrations of **DA/CPT-KK**, from 312.5 μM to 15 mM (with respect to **CPT-KK** monomer). The solutions were then filtered and washed to remove unbound antibody. Direct measurement of the fluorescein emission appeared to be much less than the balance of what was in the filtrate, likely due to quenching by the nanotubes. Therefore, we estimated the amount bound from the difference between the input and filtrate. A 1 : 1 binding model suggested a K_D of about 2.1 mM, but a higher Hill coefficient value of n_H = 2.4 provided the best fit, suggesting some cooperativity of binding (Fig. S11). Together, these results suggest relatively weak binding, consistent with the non-specific nature of the interaction, but persistent inter-

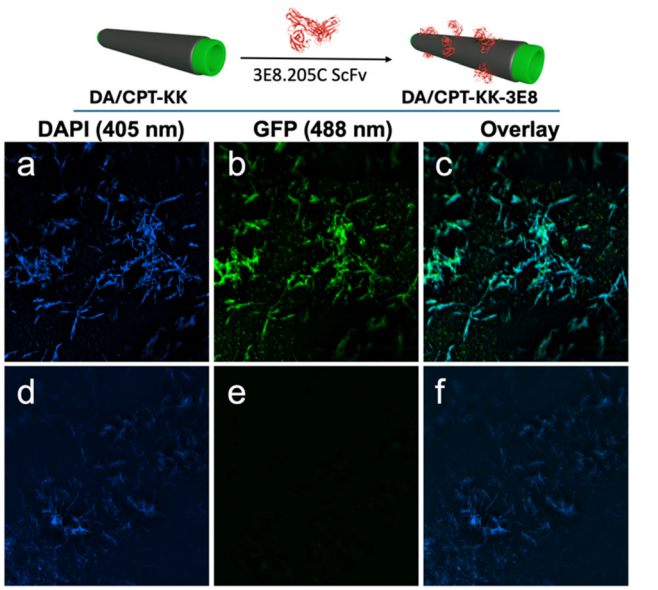

Fig. 3 Structured Illumination Microscopy (SIM) images depicting the binding of 3E8 scFv (labeled with 5% fluorescein) on surface of **DA/CPT-KK**. (a–c) Image of antibody observed in GFP channel colocalized with **DA/CPT-KK** nanotubes imaged in DAPI channel, and (d–f) without 3E8 on surface. Sample of **DA/CPT-KK-3E8** (0.63% 3E8) prepared by incubating **DA/CPT-KK** (25 μL, 10 mM) with 3E8 scFv (12.5 μL, 3.5 mg mL^{-1} in PBS) and PBS (12.5 μL) for 1 h, then filtering (0.1 μm) to remove unbound antibody.

actions that may be due to the large interaction surface (Fig. S12 and S13).

Cell viability studies showed that the presence of the targeting anti-TAG-72 scFv (3E8) on the nanotube surface significantly enhanced cytotoxicity against LS-174T colon cancer cells, which are positive for the TAG-72 antigen,[42] compared with HT-29 cells, which are thought to be negative for the antigen.[43] For example, the IC_{50} values at 96 h, measured by MTT assay, of **DA/CPT-KK** and **DA/CPT-KK-3E8** were 90 ± 10 and 42 ± 5 nM (p = 0.01), against LS-174T; and 250 ± 30 and 170 ± 90 nM (p = 0.23) against HT-29 cells, respectively. The presence of 3E8 scFv on the nanotube surface did not produce a statistically significant increase the cytotoxicity against HT-29 ($p > 0.05$), but it markedly increased toxicity against LS-174T ($p < 0.05$) (Fig. 4). As expected, exposure of both cell lines to 3E8 scFv alone showed no toxicity after 96 h, and free CPT alone was more cytotoxic. We also examined the growth of these two cell lines in the presence of **DA/CPT-KK** with and without 3E8 scFv by live cell imaging (Incucyte, Fig. S14). At multiple concentrations, HT-29 growth was unaffected by the presence of 3E8 scFv, but LS-174T showed slower growth in its presence. These data suggest that 3E8 scFv increased the effective concentration of the CPT nanotubes near TAG-72 positive cells, leading to targeted cell killing.

In summary, a modular therapeutic platform has been developed to deliver CPT to TAG-72 positive adenocarcinoma tumors. A self-assembled **CPT-KK** nanotube was coated with a conformal layer of polydopamine, resulting in a stable PDA/CPT composite nanotube with a 1.3 nm layer of PDA on the surface of the nanotube. The conformal PDA layer stabilized the nanotubes, allowing for the release of free CPT in PBS and HS, albeit at a lower rate compared to uncoated **CPT-KK** nanotubes. The adhesive PDA coating allowed for binding of the anti-TAG-72 scFv (3E8) onto the surface of the **DA/CPT-KK**-nanotubes, which showed enhanced cytotoxicity toward cell lines bearing the TAG-72 antigen. As TAG-72 does not internalize following binding by the nanotubes, it is possible that CPT enters the cell by passive diffusion after extracellular hydrolytic release. Work is ongoing to more fully understand how the nanotubes or CPT enters the cells.

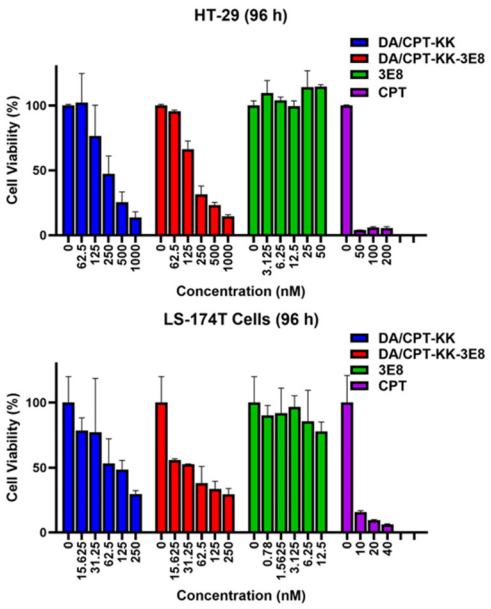

Fig. 4 MTT cytotoxicity assay on colon cancer cell lines negative (HT-29, top) and positive (LS-174T, bottom) for TAG-72 for **DA/CPT-KK**, **DA/CPT-KK-3E8**, 3E8 scFv and camptothecin (CPT). **DA/CPT-KK-3E8** exhibited greater cytotoxicity compared with **DA/CPT-KK** against LS-174T cells, but both showed similar efficacy against HT-29 cells.

Data availability

The data underlying this work are available in the published article and its SI. The supplementary information contains general synthetic, analytical and imaging methods; TEM images; binding and release studies; and live cell imaging studies. See DOI: **https://doi.org/10.1039/d5bm00788g**.

Conflicts of interest

The authors declare no competing financial interest.

Acknowledgements

This work was supported by the National Science Foundation (CHE-2106924) and by the Ralph and Marian Falk Medical Research Catalyst Award. The human serum samples were obtained commercially from Sigma and were fully deidentified from the source.

References

1 O. Afzal, A. S. A. Altamimi, M. S. Nadeem, S. I. Alzarea, W. H. Almalki, A. Tariq, B. Mubeen, B. N. Murtaza, S. Iftikhar, N. Riaz and I. Kazmi, Nanoparticles in Drug Delivery: From History to Therapeutic Applications, *Nanomaterials*, 2022, **12**, 4494.
2 H. Maeda, J. Wu, T. Sawa, Y. Matsumura and K. Hori, Tumor vascular permeability and the EPR effect in macromolecular therapeutics: a review, *J. Controlled Release*, 2000, **65**, 271–284.
3 J. Wu, The Enhanced Permeability and Retention (EPR) Effect: The Significance of the Concept and Methods to Enhance Its Application, *J. Pers. Med.*, 2021, **11**, 771.
4 M. J. Mitchell, M. M. Billingsley, R. M. Haley, M. E. Wechsler, N. A. Peppas and R. Langer, Engineering precision nanoparticles for drug delivery, *Nat. Rev. Drug Discovery*, 2021, **20**, 101–124.
5 H. Liu, Y. Y. Su, X. C. Jiang and J. Q. Gao, Cell membrane-coated nanoparticles: a novel multifunctional biomimetic drug delivery system, *Drug Delivery Transl. Res.*, 2023, **13**, 716–737.

6 E. Elhassan, N. Devnarain, M. Mohammed, T. Govender and C. A. Omolo, Engineering hybrid nanosystems for efficient and targeted delivery against bacterial infections, *J. Controlled Release*, 2022, **351**, 598–622.
7 D. Hassan, C. A. Omolo, V. O. Fasiku, C. Mocktar and T. Govender, Novel chitosan-based pH-responsive lipid-polymer hybrid nanovesicles (OLA-LPHVs) for delivery of vancomycin against methicillin-resistant Staphylococcus aureus infections, *Int. J. Biol. Macromol.*, 2020, **147**, 385–398.
8 Q. Cheng, T. Wei, L. Farbiak, L. T. Johnson, S. A. Dilliard and D. J. Siegwart, Selective organ targeting (SORT) nanoparticles for tissue-specific mRNA delivery and CRISPR-Cas gene editing, *Nat. Nanotechnol.*, 2020, **15**, 313–320.
9 S. Ruan, X. Cao, X. Cun, G. Hu, Y. Zhou, Y. Zhang, L. Lu, Q. He and H. Gao, Matrix metalloproteinase-sensitive size-shrinkable nanoparticles for deep tumor penetration and pH triggered doxorubicin release, *Biomaterials*, 2015, **60**, 100–110.
10 A. P. Singh, L. Guo, A. Verma, G. G. Wong, G. M. Thurber and D. K. Shah, Antibody Coadministration as a Strategy to Overcome Binding-Site Barrier for ADCs: a Quantitative Investigation, *AAPS J.*, 2020, **22**, 28.
11 Z. Fu, S. Li, S. Han, C. Shi and Y. Zhang, Antibody drug conjugate: the "biological missile" for targeted cancer therapy, *Signal Transduction Targeted Ther.*, 2022, **7**, 93.
12 S. M. Larson, J. A. Carrasquillo, N. K. Cheung and O. W. Press, Radioimmunotherapy of human tumours, *Nat. Rev. Cancer*, 2015, **15**, 347–360.
13 R. C. Sterner and R. M. Sterner, CAR-T cell therapy: current limitations and potential strategies, *Blood Cancer J.*, 2021, **11**, 69.
14 D. M. K. Keefe and E. H. Bateman, Potential Successes and Challenges of Targeted Cancer Therapies, *J. Natl. Cancer Inst. Monogr.*, 2019, **2019**, 25–29.
15 G. Rinnerthaler, S. P. Gampenrieder and R. Greil, HER2 Directed Antibody-Drug-Conjugates beyond T-DM1 in Breast Cancer, *Int. J. Mol. Sci.*, 2019, **20**, 1115.
16 J. T. W. Tong, P. W. R. Harris, M. A. Brimble and I. Kavianinia, An Insight into FDA Approved Antibody-Drug Conjugates for Cancer Therapy, *Molecules*, 2021, **26**, 5847.
17 S. O. Yoon, T. S. Lee, S. J. Kim, M. H. Jang, Y. J. Kang, J. H. Park, K. S. Kim, H. S. Lee, C. J. Ryu, N. R. Gonzales, S. V. Kashmiri, S. M. Lim, C. W. Choi and H. J. Hong, Construction, affinity maturation, and biological characterization of an anti-tumor-associated glycoprotein-72 humanized antibody, *J. Biol. Chem.*, 2006, **281**, 6985–6992.
18 J. Liu, R. Zhang and Z. P. Xu, Nanoparticle-Based Nanomedicines to Promote Cancer Immunotherapy: Recent Advances and Future Directions, *Small*, 2019, e1900262.
19 J. Li, R. Xing, S. Bai and X. Yan, Recent advances of self-assembling peptide-based hydrogels for biomedical applications, *Soft Matter*, 2019, **15**, 1704–1715.
20 H. Hosseinkhani, P. D. Hong and D. S. Yu, Self-Assembled Proteins and Peptides for Regenerative Medicine, *Chem. Rev.*, 2013, **113**, 4837–4861.
21 M. Ji and J. R. Parquette, Enhanced Stability of Peptide Nanofibers Coated with a Conformal Layer of Polydopamine, *Chem. – Eur. J.*, 2020, **26**, 8572–8578.
22 J. Liebscher, R. Mrowczynski, H. A. Scheidt, C. Filip, N. D. Hadade, R. Turcu, A. Bende and S. Beck, Structure of polydopamine: a never-ending story?, *Langmuir*, 2013, **29**, 10539–10548.
23 J. B. Wood, M. W. Szyndler, A. R. Halpern, K. Cho and R. M. Corn, Fabrication of DNA microarrays on polydopamine-modified gold thin films for SPR imaging measurements, *Langmuir*, 2013, **29**, 10868–10873.
24 N. E. Long, B. J. Sullivan, H. Ding, S. Doll, M. A. Ryan, C. L. Hitchcock, E. W. Martin Jr, K. Kumar, M. F. Tweedle and T. J. Magliery, Linker engineering in anti-TAG-72 antibody fragments optimizes biophysical properties, serum half-life, and high-specificity tumor imaging, *J. Biol. Chem.*, 2018, **293**, 9030–9040.
25 L. Gong, H. Ding, N. E. Long, B. J. Sullivan, E. W. Martin Jr., T. J. Magliery and M. F. Tweedle, A 3E8.scFv.Cys-IR800 Conjugate Targeting TAG-72 in an Orthotopic Colorectal Cancer Model, *Mol. Imaging Biol.*, 2018, **20**, 47–54.
26 S. H. Kim, J. A. Kaplan, Y. Sun, A. Shieh, H. L. Sun, C. M. Croce, M. W. Grinstaff and J. R. Parquette, The self-assembly of anticancer camptothecin-dipeptide nanotubes: a minimalistic and high drug loading approach to increased efficacy, *Chem. – Eur. J.*, 2015, **21**, 101–105.
27 J. H. Ryu, P. B. Messersmith and H. Lee, Polydopamine Surface Chemistry: A Decade of Discovery, *ACS Appl. Mater. Interfaces*, 2018, **10**, 7523–7540.
28 Y. Liu, K. Ai and L. Lu, Polydopamine and its derivative materials: synthesis and promising applications in energy, environmental, and biomedical fields, *Chem. Rev.*, 2014, **114**, 5057–5115.
29 H. C. Yang, R. Z. Waldman, M. B. Wu, J. Hou, L. Chen, S. B. Darling and Z. K. Xu, Dopamine: just the right medicine for membranes, *Adv. Funct. Mater.*, 2018, **28**, 1705327.
30 D. Q. Chen, L. Zhao and W. H. Hu, Protein immobilization and fluorescence quenching on polydopamine thin films, *J. Colloid Interface Sci.*, 2016, **477**, 123–130.
31 G. F. Chen, R. Y. Chen, C. X. Zou, D. W. Yang and Z. S. Chen, Fragmented polymer nanotubes from sonication-induced scission with a thermo-responsive gating system for anti-cancer drug delivery, *J. Mater. Chem. B*, 2014, **2**, 1327–1334.
32 M. S. Cartiera, K. M. Johnson, V. Rajendran, M. J. Caplan and W. M. Saltzman, The uptake and intracellular fate of PLGA nanoparticles in epithelial cells, *Biomaterials*, 2009, **30**, 2790–2798.
33 K. Cho, X. Wang, S. Nie, Z. G. Chen and D. M. Shin, Therapeutic nanoparticles for drug delivery in cancer, *Clin. Cancer Res.*, 2008, **14**, 1310–1316.
34 J. Li, C. Nagamani and J. S. Moore, Polymer Mechanochemistry: From Destructive to Productive, *Acc. Chem. Res.*, 2015, **48**, 2181–2190.
35 A. Lucas, C. Zakri, M. Maugey, M. Pasquali, P. van der Schoot and P. Poulin, Kinetics of Nanotube and Microfiber

Scission under Sonication, *J. Phys. Chem. C*, 2009, **113**, 20599–20605.

36 F. Hennrich, R. Krupke, K. Arnold, J. A. R. Stutz, S. Lebedkin, T. Koch, T. Schimmel and M. M. Kappes, The mechanism of cavitation-induced scission of single-walled carbon nanotubes, *J. Phys. Chem. B*, 2007, **111**, 1932–1937.

37 M. Ji, B. Daniels, A. Shieh, D. A. Modarelli and J. R. Parquette, Controlling the length of self-assembled nanotubes by sonication followed by polymer wrapping, *Chem. Commun.*, 2017, **53**, 12806–12809.

38 C. D. Jones and J. W. Steed, Gels with sense: supramolecular materials that respond to heat, light and sound, *Chem. Soc. Rev.*, 2016, **45**, 6546–6596.

39 M. Ji, B. Daniels, A. Shieh, D. A. Modarelli and J. R. Parquette, Controlling the length of self-assembled nanotubes by sonication followed by polymer wrapping, *Chem. Commun.*, 2017, **53**, 12806–12809.

40 Y. Sun, C. M. Fry, A. Shieh and J. R. Parquette, Self-assembly of a robust, reduction-sensitive camptothecin nanotube, *Chem. Commun.*, 2020, **56**, 10337–10340.

41 G. L. Beretta and F. Zunino, Relevance of extracellular and intracellular interactions of camptothecins as determinants of antitumor activity, *Biochem. Pharmacol.*, 2007, **74**, 1437–1444.

42 H. M. Hollandsworth, S. Amirfakhri, F. Filemoni, R. M. Hoffman, J. Molnar, P. J. Yazaki and M. Bouvet, Humanized Anti-Tumor-Associated Glycoprotein-72 for Submillimeter Near-Infrared Detection of Colon Cancer in Metastatic Mouse Models, *J. Surg. Res.*, 2020, **252**, 16–21.

43 L. Chen, Y. Wang, X. Liu, S. Dou, G. Liu, D. J. Hnatowich and M. Rusckowski, A new TAG-72 cancer marker peptide identified by phage display, *Cancer Lett.*, 2008, **272**, 122–132.